Accepted Manuscript

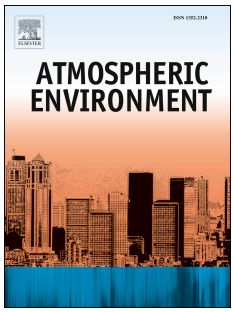

Spatial and temporal distribution of NO_2 and SO_2 in Inner Mongolia urban agglomeration obtained from satellite remote sensing and ground observations

Caiwang Zheng, Chuanfeng Zhao, Yanping Li, Xiaolin Wu, Kaiyang Zhang, Jing Gao, Qi Qiao, Yuanzhe Ren, Xi Zhang, Fahe Chai

PII: S1352-2310(18)30412-6

DOI: 10.1016/j.atmosenv.2018.06.029

Reference: AEA 16087

To appear in: *Atmospheric Environment*

Received Date: 19 March 2018

Revised Date: 15 June 2018

Accepted Date: 17 June 2018

Please cite this article as: Zheng, C., Zhao, C., Li, Y., Wu, X., Zhang, K., Gao, J., Qiao, Q., Ren, Y., Zhang, X., Chai, F., Spatial and temporal distribution of NO_2 and SO_2 in Inner Mongolia urban agglomeration obtained from satellite remote sensing and ground observations, *Atmospheric Environment* (2018), doi: 10.1016/j.atmosenv.2018.06.029.

Spatial and Temporal Distribution of NO_2 and SO_2 in Inner Mongolia Urban Agglomeration Obtained from Satellite Remote Sensing and Ground Observations

Caiwang Zheng[1], Chuanfeng Zhao[1,3]*, Yanping Li[2*], Xiaolin Wu[1], Kaiyang Zhang[1], Jing Gao[4], Qi Qiao[2], Yuanzhe Ren[5], Xi Zhang[2], Fahe Chai[2]

1. State Key Laboratory of Earth Surface Processes and Resource Ecology, and College of Global Change and Earth System Science, Beijing Normal University, Beijing 100875, China

2. Chinese Research Academy of Environmental Sciences, Beijing, 100012, China

3. Division of Geological and Planetary Sciences, California Institute of Technology, Pasadena, CA 91125, USA.

4. Rinpoche (Beijing) Technology Co., Ltd, Beijing, 100094, China

5. The Inner Mongolia Autonomous Region Environmental Monitoring Center Station, Hohhot, 010011, China

Correspondence to: Chuanfeng Zhao, czhao@bnu.edu.cn;

Yanping Li, leeyp@craes.org.cn

Abstract: Nitrogen dioxide (NO_2) and sulfur dioxide (SO_2) are important pollution gases which can affect air quality, human health and even climate change. Based on the combination of tropospheric NO_2 and SO_2 column density products derived from OMI satellite with the ground station observations, this study analyzed the spatial-temporal distribution of NO_2 and SO_2 amount in Inner Mongolia urban agglomerations. It shows that NO_2 increased continually from 2005 to 2011 at a rate of 14.3% per year and then decreased from 2011 to 2016 at a rate of -8.1% per year. SO_2 increased from 2005 to 2007 with a rate 9.7% per year. While with a peak value in 2011, SO_2 generally showed a decreasing trend of -1.6% per year from 2007 to 2016. With regard to the spatial pattern, the highest levels of NO_2 occur in Hohhot and Baotou, followed by Wuhai and Ordos, the least in Bayannur. Compared with NO_2, the spatial distribution of SO_2 is slightly different. The pollution of SO_2 is the most serious in Wuhai, followed by Hohhot and Baotou, and the lightest in Ordos and Bayannur. The diurnal variations of NO_2 and SO_2 are basically the same, which decrease from 0:00 to 6:00, then increase to a peak value at 8:00, and decrease from 8:00 to 15:00. The diurnal variation of NO_2 and SO_2 is highly related to the diurnal variation of both anthropogenic emission and boundary layer height. Differently, the long-term spatial-temporal distribution of NO_2 and SO_2 are more closely related to human activities.

Keywords: NO_2; SO_2; OMI; Inner Mongolia; long-term trend; spatial distribution

Highlights

(1) Long-term spatial-temporal distribution of NO_2 and SO_2 amount in Inner Mongolia urban agglomerations were analyzed.

(2) Both NO_2 and SO_2 show increasing and then decreasing temporal trend, but with different turning time which are 2007 and 2011, respectively.

(3) NO_2 and SO_2 show slightly different spatial distributions, with the highest concentration in Hohhot and Baotou for NO_2 and Wuhai for SO_2.

1. Introduction

In the past decades, coupled with China's burgeoning economy is the terrible air pollution (Chan and Yao, 2008), which is mainly caused by China's industrial explosive growth and urbanization development. Air pollutants can be divided into two forms, particulate matter (PM) and gaseous pollutants. PM has attracted great public concern because of its severe health impact (Yuan et al., 2012; Chang et al., 2012), especially for cardiovascular and respiratory disease, as well as reduced visibility caused by smog. Gaseous pollutants, such as sulfur dioxide (SO_2), nitrogen dioxide (NO_2), and ozone (O_3), also play very important roles in our atmospheric environment and get more and more attentions (Hao et al., 2007; Wang et al., 2011).

NO_2 and SO_2 are both important trace gases and play a significant role in the complex atmospheric chemistry process of the troposphere, causing a series of urban environmental pollution problems such as acid rain, haze and photochemical smog (WHO, 2000; IPCC, 2007; He et al., 2007; Shon et al., 2011). The secondary sulfate and nitrate particulate is formed by oxidation of gas granules, contributing to the particle concentration in the air and thus influencing the radiative budget and climate (Kajino et al., 2011). They can also promote the formation of acid rain and cause the decrease of crop yields and destruction of ecology (Richter et al., 2006; Dickerson et al., 2007). NO_2 is primarily released by anthropogenic emissions, which contain the industrial burning of fossil fuels such as coal, oil and gas, vehicle exhaust, biomass burning, and electricity generation. In terms of natural sources, it is emitted from soils through the decomposition process of nitrates and can also be produced by lightning (Richter and Burrows, 2002; Cheng et al., 2012). Similarly, SO_2 is released into the atmosphere through both natural and anthropogenic emissions. Natural sources mainly refer to volcanic eruptions while anthropogenic sources include the burning of

fossil fuels containing sulfur for domestic heating and the power generation for industrial activities (Zhang et al., 2017).

Over the years, researchers began to realize the detrimental effects of NO_2 and SO_2 to human health and plants, thus carried out studies about these two polluted gases (Ul-Haq et al., 2015). Compared with traditional ground station measurements which can provide continuous observations of near surface pollutants for a long time, satellite remote sensing offers other advantages, such as a coverage of large area with high spatial continuity. The satellite observations allow us to study the long-term spatio-temporal distribution of NO_2 and SO_2, the characteristics of long-distance transport (Zhang et al., 2008), as well as the pollutant contribution from various sources (Wang et al., 2012; Lu et al., 2013). To effectively acquire information of atmospheric pollutants, a lot of on-board satellite instruments are designed, such as Global Ozone Monitoring Experiment (GOME), SCanning Imaging Absorption spectroMeter for Atmospheric CHartographY (SCIAMACHY), GOME-2 and Ozone Monitoring Instrument (OMI). OMI is widely used and has high spatial and temporal resolution (Krotkov et al., 2016; Levelt et al., 2018). As overviewed by Levelt et al. (2018), OMI has been applied to various study themes including air quality monitoring, detection of ozone, volcanoes, spectral solar radiation, and so on. For air quality monitoring, OMI can provide information of several key pollutants such as NO_2, SO_2, aerosols, and HCHO. Damiani et al. (2012) used the ground-based total ozone measurements from 2007 to 2009 in the Arctic to check the quality of OMI, GOME and SCIAMACHY satellite-based data, and found that there was a good agreement between satellite- and ground-based observations despite of some systematic biases. Ul-Haq et al. (2015) investigated temporal trends, seasonality, and anomalies of tropospheric NO_2 pollution over four basins in South Asia using OMI

measurements during the period 2004-2015. Lamsal et al. (2015) quantified the NO_2 temporal trend from 2005 to 2013 over the United States using surface measurements and tropospheric NO_2 vertical column density (VCD) data from OMI products. Krotkov et al. (2016) expanded the study area and used the OMI observation to investigate the SO_2 and NO_2 pollution changes over different countries of the world for the period of 2005 to 2014.

There are also many studies regarding the OMI-observed SO_2 and NO_x emission trends over China (van der A et al., 2016; Liu et al., 2016, 2017; Cui et al., 2016; Li et al., 2010, 2017; Zhang et al., 2017). Li et al. (2010) found the large reduction of SO_2 emissions from Chinese power plants in 2005-2007 based on OMI observations, and Li et al. (2017) indicated that SO_2 emission have declined by 75% in China since 2007 using OMI observations, making China surpassed by India for the total anthropogenic SO_2 emissions. Liu et al. (2016) investigated the temporal variation of NO_x over China at a national level based on both OMI observations and emission inventories, and they found a deceasing trend of column NO_2 by 32% from 2011 to 2015. Liu et al. (2018) further investigated the NO_x emissions from 48 cities and seven power plants over China, and found an increase by 52% from 2005 to 2011 and a decrease by 21% from 2011 and 2015 based on OMI observations. van der A et al. (2016) studied the air quality trends from 2005 to 2015 and evaluated the effectiveness of air quality policy for SO_2 and NO_x emissions in China. Zhang et al. (2017) analyzed the long-term trend of spatial and temporal distribution of NO_2 and SO_2 column density in Henan Province using OMI product. Cui et al. (2016) indicated that western China experienced rapid growth of NO_2 during 2005-2013, including the Inner Mongolia city cluster region. Note that Cui et al. (2016) mainly focused on regional statistical study of NO_2 from 2005 to 2013 for several regions in western

China. By contrast, there is no intensive study for the gaseous pollution of SO_2 and NO_2 with high city/county level resolution over the Inner Mongolia region so far.

Inner Mongolia accounts for 12.3% of the land area in China and is rich in natural resources, of which coal reserves rank the second place among thirty-four provinces in China, making it become China's important energy heavy chemical base (NBS, 2013). Industries such as thermal power, chemical engineering and metallurgy impose a heavy burden on air quality. Various types of air pollutants have been increasing in recent years. Particularly, the amount of coal burning has increased greatly in winter heating period, making the air quality worse. As indicated by Cui et al. (2016), the increasing trend rate of NO_2 in 2005-2013 is as high as 10.2±1.3% per year for the Inner Mongolia region. Currently, the first pollution-contributing factor is particulate matter, which is mainly from natural coal ash emission, dust and automobile exhaust emissions; and the second is SO_2 (IMESB, 2006). How to make a balance between the energy structure modulation and the improvement of air quality is an essential issue for public interests. To do that, we first need to obtain detailed pollution status over this region, such as SO_2 and NO_2. Therefore, this study aims to investigate the long-term trend and spatial distribution characteristics of NO_2 and SO_2 in Inner Mongolia urban agglomerations using both OMI measurements and ground-station observations.

The paper is organized as follows. Section 2 describes the data and method. Section 3 analyzes the spatial-temporal trends of NO_2 and SO_2 at cities in Inner Mongolia, and section 4 summarizes the findings.

2. Data and Method

2.1 Study region

Inner Mongolia is the third largest province in China, with an area of about 1,183,000 km^2, population of 25 million, and Gross Domestic Product (GDP) of 1.78 trillion RenMinBi (RMB) in 2015 (CSY, 2015). From 2006 to 2011, the GDP growth rate was between 15% and 20% (generally ~15%) per year while it is about 7% after 2011 because of the adjustment of economic policy.

The study region is located in the core area of the middle and western Inner Mongolia, including Hohhut, Baotou, Ordos, Bayannur and Wuhai. Relying on abundant coal and natural gas resources, Hohhut-Baotou-Ordos (H-B-O) agglomeration has become the most dynamic economic circle in Inner Mongolia autonomous region. Hohhut is the capital city; Baotou is the largest city of Inner Mongolia; and Ordos is an emerging prairie city with rich energy resources. As shown in Figure 1, Hohhut, Baotou and Ordos are situated in the Hetao plain with Yinshan mountain on the northern area, whereas Bayannur and Wuhai are in the ordos plateau. The difference of topography may influence the transport of air pollutants. In this study, we assume that natural contribution is roughly uniform in space (cities) and time while some uncertainties could be introduced. Generally, the anthropogenic emissions of NO_2 and SO_2 are much larger than natural contributions in these cities. By investigating the spatio-temporal distribution of NO_2 and SO_2 in these representative cities, we can evaluate the influence of human activities on the air quality of Inner Mongolia during past few years.

2.2 Aura satellite and OMI

Aura is a sun-synchronous orbit satellite tracking at 705 km altitude and crossing

171 the equator at about 13:45 local time (LT), which was launched on July 15, 2004
172 (OMI Data User's Guide, 2012). It aims for observations and studies of the air quality,
173 the ozone layer of earth, and climate change. OMI is a nadir pointing hyper-spectral
174 imaging sensor aboard Aura spacecraft with a spatial resolution of 13 km×24 km. It
175 covers the whole earth once a day and provides the measurements of ozone profile,
176 NO_2, SO_2, aerosol, cloud, as well as the trace gases such as HCHO, BrO and OClO.

177 Both Level 2 and daily Level 3 product of the planetary boundary layer (PBL)
178 SO_2 and tropospheric NO_2 vertical column density (VCD) data were employed in this
179 study. The VCD is defined as the amount of molecules for a specific atmospheric gas
180 from the surface to the height indicated, such as the instrument height (Lamsal et al.,
181 2015). The Level 2 (orbital swaths) product has individual files for each orbit of data
182 at a spatial resolution of 13 kmx24 km, while the Level 3 product is a gridded data on
183 uniform space-time scales with a 0.25°×0.25° spatial resolution and daily time
184 resolution (Eskes and Boersma 2003, Boersma et al., 2011). The Level 2 product
185 provides instantaneous NO_2 and SO_2 data which can be used to match the surface site
186 hourly observations, while the Level 3 product are processed daily gridded data,
187 which is more suitable for long-term trend analysis. Therefore, in this study, the
188 former is used for the comparison with the ground-based observations and the latter is
189 applied to the analysis of spatial distribution and long-term spatial-temporal trend of
190 NO_2 and SO_2 over the Inter-Mongolia region.

191 **2.3 Ground station observations and pollution emission**

192 Since January 2013, the Ministry of Environmental Protection of China began to
193 publicize real time monitoring data of 6 major pollutants over 74 cities, which include
194 $PM_{2.5}$, PM_{10}, O_3, SO_2, NO_2 and CO respectively. This dataset has been used in many

195 studies and can be obtained from http://datacenter.mep.gov.cn/ (Ma et al. 2014; Chen
196 et al., 2015). In our study, we adopted hourly NO_2 and SO_2 mass concentrations from
197 2014 to 2016 in five cities of Inner Mongolia, which are provided by Inner Mongolia
198 Municipal Environmental Protection. There are totally 31 monitoring stations,
199 including 10 sites in Hohhut, 7 sites in Baotou, 3 sites in Ordos, 6 sites in Bayannur
200 and 5 sites in Wuhai, which are shown in Fig. 1. These data are used for the
201 evaluation of satellite observations and analysis of seasonal and diurnal variation of
202 near-surface NO_2 and SO_2 concentrations.

203 To study the influence of the emission source on the air quality, we collected
204 data on two aspects from the China Statistical Yearbook: one is the consumption data
205 of various types of energy, such as coal, fuel and gas; the other is the emission data of
206 gaseous pollutants from industrial and domestic activities, which includes NO_2, SO_2
207 and smoke. This data can be downloaded from http://www.stats.gov.cn/tjsj/ndsj/.

208 **2.4 Meteorological data**

209 The washout process of rainfall on NO_2 and SO_2 in the atmosphere can reduce
210 the air pollution near the surface, in addition to producing acidic precipitation. To
211 study the seasonal variation characteristics of precipitation and its potential effect on
212 surface air pollution in Inner Mongolia, we use China Hourly Merged Precipitation
213 Analysis (CMPA) product from 2014 to 2016. The CMPA product has merged
214 observations from automatic weather stations with Climate Precipitation Center
215 Morphing (CMORPH) product based on the probability density function–optimal
216 interpolation (PDF-OI) methods, with a spatial resolution of 0.1° x 0.1°. The overall
217 error of this dataset is within 10% and the errors for regions with heavy rainfall or
218 sparse ground sites are less than 20% (Shen et al., 2014). The surface solar radiation

downwards (SSRD) and planetary boundary layer height (PBLH) are extracted from the European Centre for Medium-Range Weather Forecasts (ECMWF) interim reanalysis (ERA-Interim; Dee et al., 2011), with a horizontal resolution of 0.125° x 0.125° and 3 h temporal resolution.

3. Analysis and Results

3.1 Comparison between satellite and ground observations

Considering that satellite observations have much coarser temporal and spatial resolution than the ground observations, we generally need carry out the spatial-temporal matching, which figures out the spatial domain with satellite observation average more comparable to the surface measurements and the time range with the surface observation average more comparable to the satellite measurements. Spatial-temporal matching is an essential condition for the comparison between satellite and ground observations since it can reduce the errors caused by the temporal change and spatial heterogeneity of NO_2 and SO_2. As for the spatial matching, the spatial averaged OMI VCD NO_2 and SO_2 within 100, 50, 30 and 10 km radius regions surrounding the surface monitoring station as the center were compared to the ground observed values, and it shows that when the radius is 30 km, the observations from satellite have the highest consistency with those from surface stations. Therefore, we used 30 km as a critical value for the regional average of satellite observations. Note that we only tested the domains with 100, 50, 30 and 10 km radius, domain with another value radius could be more suitable while not tested. With regard to temporal matching, only when the OMI data is available, the corresponding ground-observed NO_2 and SO_2 in time within 30-min of the satellite overpass time are compared to OMI measurements. Figure 2 shows the comparison of NO_2 and SO_2 between

monthly averaged OMI VCD products scaled by planetary boundary layer height (PBLH) and the ground-based measurements using the data from 2014 to 2016 in Inner Mongolia. PBLH is likely the most important factor to the vertical distribution of NO_2 and SO_2. In general, NO_2 and SO_2, along with fine aerosol particles, mainly concentrate within PBLH. Moreover, the planetary boundary layer is a well-mixed layer in which NO_2 and SO_2 vary weakly with heights. We could consider the impacts of vertical profile on our inter-comparison roughly by using PBL scaled column NO_2 and SO_2 (VCD NO_2/PBL and VCD SO_2/PBL), making them more comparable to the ground based measurements of NO_2 and SO_2 concentration. Overall, the correlations are high, with R^2 of 0.80 for NO_2 and 0.48 for SO_2. It demonstrates that the satellite is an effective way to monitor the monthly-averaged characteristics of surface SO_2 and NO_2. However, when using daily measurements, the correlations between satellite and ground station observations for both SO_2 and NO_2 are low, which can be attributed to multiple reasons. First, the gridded OMI product represents an averaged NO_2 and SO_2 status of a region while the ground station reflects the status at a single site. Noting that anthropogenic pollutants could serve as a dominant contributing source in addition to the contribution from natural emissions (Cui et al., 2016), the spatial heterogeneity of pollutants caused by the emission difference and meteorological condition makes R^2 not very high. Second, the influence of cloud and aerosol can bring uncertainties to the OMI retrievals to some extent. In addition, the lack of more precise consideration for the vertical profile of NO_2 and SO_2 could lead to noticeable errors in the comparison between the surface concentrations and satellite-observed columns. For example, Lamsal et al. (2015) indicated up to 15% errors in the temporal trend estimation of NO_2 emission when using OMI column NO_2.

3.2 Spatial and temporal distribution of NO_2 and SO_2

Figure 3 describes the spatial distribution of satellite- and ground-based NO_2 and SO_2 averaged for the period from 2014 to 2016 in Inner Mongolia urban agglomerations. It shows that highly polluted areas are concentrated in the cities with industrial clusters while the suburbs are less polluted. In terms of the spatial distribution of NO_2, the highest levels of pollution occur in Hohhot and Baotou, followed by Wuhai and Ordos, the least polluted area in Bayannur. Compared with NO_2, the SO_2 spatial distribution is slightly different. The pollution of SO_2 is the most serious in Wuhai, followed by Hohhot and Baotou, and the lightest in Ordos and Bayannur. In general, Bayannur has a better air quality and the SO_2 amount in Wuhai is much larger than that in other cities, with a multi-year average value of 67 $\mu g/m^3$. It was shown that the SO_2 emission intensity per unit area of Wuhai is 33 times as much as the national average level in 2015, which is much higher than other coal-producing cities (NIW, 2017). High SO_2 pollution in Wuhai can be attributed to several factors, including unreasonable industrial layout, industrial recovery, spontaneous combustion of coal seam and special topography and climate conditions (NIW, 2017), which has attracted the attention of Wuhai municipal government for recent years. Overall, both satellite and ground observations show similar results regarding the heavily, moderately and slightly polluted regions. Fig. 3 also reveals the superiority of satellite remote sensing observations in large spatial scale analysis of air pollution.

Figure 4 shows both monthly and seasonal variations of VCD NO_2, VCD SO_2 and rain rate from 2005 to 2016 in Inner Mongolia. The monthly averaged VCD NO_2 and SO_2 show periodic changes with one year as a cycle, reaching its maximum values in winter and minimum values in summer. The rain rate also shows a one-year periodic change. However, the seasonal variation of rain rate is opposite to that of

292 VCD NO_2 and VCD SO_2, which may be partly due to the fact that the wet deposition
293 of precipitation can significantly reduce the amount of pollutants in the atmosphere
294 (Feng et al., 2001). In other words, abundant precipitation caused by summer
295 monsoon could be an important factor contributing to low NO_2 and SO_2 in summer.
296 Another important influential factor to the seasonal variation of VCD NO_2 and SO_2 is
297 the more serious emissions in cold winter period.

298 Fig. 4 also shows that there are different temporal trends for both monthly and
299 seasonally averaged VCD NO_2 between before and after 2011. Before 2011, there is a
300 clear increasing trend in the monthly and seasonally averaged VCD NO_2 with an
301 increasing rate of 1.1% per month. After 2011, the trend has become decreasing with
302 time. Differently, the monthly and seasonally averaged VCD SO_2 shows a turning
303 change in the temporal trends in 2007 instead of 2011. The VCD SO_2 increased with
304 time before 2007, and decreased with time after 2007. To further examine this, Figure
305 5 shows the temporal variation of annually averaged VCD NO_2 and SO_2, which
306 divides all time into two periods, one with an increasing and the other with a
307 decreasing trend. For NO_2, it goes up from ~1.7×10^{15} in 2005 to ~3.5×10^{15}
308 (molecules/cm^2) in 2011 with an increasing rate of ~14.4% per year except a slight
309 decline in 2008, which may be caused by pollution control and mitigation measures
310 for the 2008 Olympic Games. However, the period of 2011 to 2016 witnesses a
311 noticeable downward trend for NO_2 with a decreasing rate of ~8.1% per year. In
312 contrast, the SO_2 increases from ~0.32 in 2005 to ~0.37 (D.U.) in 2007 with an
313 increasing rate of ~9.7%. For the period from 2007 to 2016, it shows a general
314 downward trend with a decreasing trend of ~1.6% despite of a great upswing in 2011.

315 It is expected that the spatial and temporal trends of NO_2 and SO_2 should be
316 closely associated with the energy consumption structure and exhaust emissions over

the study areas. Figure 6 shows the annual variation of the NO_2 and SO_2 emissions from China and Inner Mongolia, along with the annual variation of consumption of energy in Inner Mongolia (Table 1). Inner Mongolia has served as the energy and heavy-chemistry base of China for a long time. Coal is the main energy resource for Inner Mongolia, accounting for more than 94% of the energy consumption of the industry (NBS, 2013). The consumption of fossil fuel keeps a consistent increase with a growth rate of 14.8% for coal and 18.1% for fuel from 2005 to 2011 and then decreases from 2012 to 2015 despite of slight fluctuations. However, the emission of SO_2 shows a general declining trend due to the economic policy adjustment and technical improvement.

The 11^{th} Five Year Plan (FYP) which was issued in 2005 requires that the emission of SO_2 decline 3.2% in 2010 according to the environmental protection goal (IMESB, 2006). To meet the goal, the traditional coal fired boilers have been modified or abandoned. Meanwhile, a lot of waste gas treatment facilities were installed to realize the flue gas desulfurization (FGD), making the SO_2 removal rate increase from 24.1% in 2006 to 57.3% in 2010. In 2007, Inner Mongolia's total SO_2 emission was about 145.59 million tons (88% from industrial activities) and ranked 4^{th} in China. By contrast, it was reduced by 6.19 million tons in 2010. Due to the economy resurgence, a temporary recovery of SO_2 emission was done in 2011 with a growth rate of 0.86% compared with 2010, which is consistent with the trend observed in Fig. 5(b). After that, the SO_2 emission decreased continuously and reduced by 17.85 million tons in 2015.

The energy consumption keeps going up for the sake of rapid economic development in Inner Mongolia during the period from 2006 to 2015. Correspondingly, the NO_2 emission grows up strikingly from 89.82 in 2006 to 129.38

342 million tons in 2010, with an annual growth rate of 8.8%. One likely reason is that the
343 removal rate of NO_x in industrial processes is generally low with a rate of 2.9%. The
344 China 12th FYP policy is expected to realize 10% NO_x reduction compared to the 2010
345 level in 2015. Ambient air quality standards (GB3095-2012) was announced which
346 require traffic, agricultural and industrial coordinated emission reduction. Moreover,
347 more and more clean energy are being used in Inner Mongolia, such as the
348 establishment of wind farms. The usage of alternative energy may promote the
349 transformation and optimization of industrial structure, contributing to the
350 improvement of urban air quality in the future. As a result, NO_2 emission decreased
351 significantly by 28.3 million tons in 2015. As is shown in Fig. 6, the temporal
352 changing trend of NO_2 and SO_2 emissions in China is roughly consistent with that in
353 Inner Mongolia.

354 Figure 7 further shows the spatial distributions of biennial averaged VCD NO_2
355 and SO_2 from 2005 to 2016 in Inner Mongolia urban agglomerations. The high
356 polluted hotspots of VCD NO_2 are mainly centralized in areas with high population,
357 industrialization, urbanization and agricultural activities. From 2005 to 2011, the NO_2
358 pollution area surrounding key cities is expanding and the pollution level is rising,
359 which is consistent with the increase of NO_2 emission shown in Fig. 6. Nevertheless,
360 the NO_2 pollution over the areas around the cities becomes to decrease with time from
361 2012. Differently, the biennial averaged VCD SO_2 increases slightly from 2005-2006
362 to 2007-2008, and then experiences a continuous decrease with time from 2007. This
363 is also roughly consistent with the temporal trend of SO_2 emission amount in this
364 region as shown in Fig. 6.

3.3 Pollution over five cities

Figure 8 shows the monthly averaged surface NO_2 and SO_2 in five cities, and rain rate and SSRD over the Inner Mongolia. Overall, the monthly variation of NO_2 and SO_2 concentrations presents a "U" shape curve, with peaks in winter and valleys in summer. Emission source is one of the main factors leading to this seasonal variation, along with the seasonal changes of chemical lifetime of NO_2 and SO_2, planetary boundary layer height, precipitation and other meteorology variables. For the emission source, coal-fired heating emissions in winter should be an important contributing factor. In addition, it has been figured out that the lifetime of NO_x in winter is several times longer than in summer (Cui et al., 2016), and the lifetime of SO_2 in winter (58±20 hours) is also a few times longer than in summer (19±7 hours) (Lee et al., 2011). This seasonal variation of lifetime will contribute to higher NO_2 and SO_2 concentration in winter than in summer. Fig. 8(c-d) demonstrate that both rain days and SSRD show an opposite monthly variation compared to that of NO_2 and SO_2. In summer, the wet scavenging of precipitation can significantly reduce the concentration of atmospheric pollutants. Also, the high temperature and relative humidity in summer atmosphere are beneficial to the removal of NO_2 through photolysis (Feng et al., 2001; Dong et al., 2009). By contrast, in winter, radiation reaching on the ground is less and the boundary layer decreases a lot, causing the build-up of near surface air pollutants and thus more serious air pollution.

Figure 9 shows the diurnal variation of surface NO_2 and SO_2 concentrations at five cities in Inner Mongolia for the period from 2014 to 2016. In general, the SO_2 shows a bimodal pattern with a flat "W" shape for the diurnal cycle in all five cities except for Wuhai. For most cities other than Wuhai, the lowest SO_2 concentration appears at around 3:00-5:00 LT and 15:00-19:00 LT while the peak appears at about

8:00-11:00 LT and 20:00-24:00 LT, which is highly related to the human activities and meteorological condition. Obviously, during the period from 6:00 to 8:00 LT, anthropogenic activities start, and a combination of vehicle exhaust fumes and factory waste gases result in the growth of SO_2 concentration. However, from 9:00 to 16:00 LT, with the increase of solar radiation reaching the surface, the turbulence and exchange of pollutants in the vertical direction of atmosphere become more active, resulting in much higher boundary layer, less accumulation of near-surface pollutants, and thus lower SO_2 concentrations.

Different from other four cities, SO_2 concentration in Wuhai shows a single mode diurnal variation with maximum values around 9:00 LT and minimum values around 18:00 LT. Moreover, Wuhai suffers more SO_2 with a peak value reaching 100 $\mu g/m^3$. This could be associated with its industrial structure and urban layout. Heavy industry for power and heat generation, petroleum processing, coke making, and so on, produces serious SO_2 emissions. Meanwhile, the industrial zone is mainly distributed in the south area of Wuhai which is on the upwind direction of the urban district for most time (Chen, 2014).

The diurnal variation of NO_2 shows the similar bimodal distribution as that for SO_2. Differently, NO_2 over all five cities shows the maximum values around 8:00-9:00 LT and 19:00-22:00 LT, and the minimum values around 5:00 LT and 15:00 LT. From 9:00 to 15:00 LT, associated with the increase of solar radiation, the boundary layer height rises and the photochemical reaction process of NO_2 and volatile organic compounds (VOC) to O_3 increases, resulting in the decreasing trend of NO_2 concentrations (Duncan et al., 2010). The night time decrease of NO_2 from 22:00 to 5:00 LT could be related to the reduced anthropogenic activities (e.g., vehicles) during this period. It's worth noting that the air quality of Ordos is relatively

415 better than that of other cities with SO_2 and NO_2 both lower than 30 μg/m^3.

416 **4. Summary**

417 Combing NO_2 and SO_2 column density product derived from OMI satellite with
418 the surface concentrations from ground station observations, this study analyzed the
419 spatial-temporal distribution characteristics of NO_2 and SO_2 in the Inner Mongolia
420 urban agglomeration. While there are numerous studies about the spatio-temporal
421 variation of NO_2 and/or SO_2 in China based on OMI satellite observations, this study
422 provides unique information for both NO_2 and SO_2 from 2005 to 2016 at a city scale
423 over Inner Mongolia.

424 In terms of long-term changing trend, NO_2 increased continually from 2005 to
425 2011 at a rate of 14.3% per year and then decreased from 2011 to 2016 at a rate of
426 8.1% per year. Differently, there is a consistent increase for SO_2 from 2005 to 2007 at
427 a rate of 9.7% per year. During the period from 2007 to 2016, despite of a peak value
428 in 2011, it showed a decreasing trend for SO_2 at a rate of 1.6% per year.

429 As for the spatial pattern of NO_2, the highest levels of pollution occur in Hohhot
430 and Baotou, followed by Wuhai and Ordos, the least polluted area in Bayannur.
431 Compared with NO_2, the SO_2 spatial distribution is slightly different. The pollution of
432 SO_2 is the most serious in Wuhai, followed by Hohhot and Baotou, and it is the
433 lightest in Ordos and Bayannur.

434 The diurnal variation of NO_2 and SO_2 is basically the same, which shows
435 bimodal pattern with a flat “W” shape, particularly for cities other than Wuhai. This
436 type of diurnal variation of NO_2 and SO_2 is highly related to the diurnal variation of
437 anthropogenic emission and boundary layer height. The long-term spatial-temporal
438 distributions of NO_2 and SO_2 are closely related to human activities, while

meteorology also plays an important role for their diurnal and seasonal variations.

Overall, the adjustment of the urban energy structure, such as the reduction of fossil energy use and the promotion of clean energy development, and the installment of waste gas treatment facilities contribute to the decrease of NO_2 and SO_2 emissions in recent years. Therefore, the air quality in Inner Mongolia has generally improved over the past few years. However, the turning year from increasing trend to decreasing trend is different for NO_2 and SO_2. Moreover, the SO_2 pollution situation in Wuhai is still very serious and additional efforts should be made to fully control and govern air pollution caused by human activities.

Acknowledgements: This work was supported by the Environmental Protection Department (EPD) (grant number 201509020), the National Natural Science Foundation of China (grant 41575143), the State Key Laboratory of Earth Surface Processes and Resource Ecology (2017-ZY-02), the China “1000 plan” young scholar program, the Fundamental Research Funds for the Central Universities (2017EYT18, 312231103).

References

Boersma, K. F., Eskes, H. J., Dirksen, R. J., Veefkind, J. P., Stammes, P., Huijnen, V., Kleipool, Q. L., et al. 2011. An Improved Tropospheric NO_2 Column Retrieval Algorithm for the Ozone Monitoring Instrument. Atmospheric Measurement Techniques; 4: 1905–1928, doi:10.5194/amt-4-1905-2011.

Chen, W., Tang, H., Zhao, H., 2015. Diurnal, weekly and monthly spatial variations of air pollutants and air quality of Beijing. Atmos. Environ; 119, 21-34, http://dx.doi.org/10.1016/j.atmosenv.2015.08.040.

463 Chan, C.K., Yao, X., 2008. Air pollution in mega cities in China. Atmospheric
464 Environment; 42: 1-42.

465 Chang, Y., 2012. China needs a tighter $PM_{2.5}$ limit and a change in priorities.
466 Environmental Science & Technology; 46: 7069-7070.

467 Chen, X., Bai, J., 2014. Study on the air pollution characteristics of Wuhai urban
468 district and its coutermeasures for control. Environment and Development; 26
469 (3): 31-33.

470 Cheng, M., Jiang, H., Guo, Z., 2012. Evaluation of long-term tropospheric NO_2
471 columns and the effect of different ecosystem in Yangtze River Delta. IEEE
472 International Symposium on Geoscience and Remote Sensing IGARSS; pp.
473 2501-2504.

474 CSY, 2015. China Statistical Yearbook. China Statistical Publishing House, Beijing.

475 Cui, Y., Lin, J., Song, C., Liu, M., Yan, Y., Xu, Y., and Huang, B., 2016. Rapid growth
476 in nitrogen dioxide pollution over Western China, 2005-2013. Atmos. Chem.
477 Phys., 16, 6207-6221.

478 Damiani, A., De Simone, S., Rafanelli, C., Cordero, R.R., Laurenza, M., 2012. Three
479 years of ground-based total ozone measurements in the Arctic: Comparison
480 with OMI, GOME and SCIAMACHY satellite data. Remote Sensing of
481 Environment; 127: 162-180.

482 Dong, J., Wang, S., Shang, K., 2009. Influence of precipitation on air quality in
483 several cities of China. Journal of Arid Land Resources and Environment; 23(12):
484 43:48.

485 Dickerson, R.R., Li, C., Li, Z., Marufu, L.T., Stehr, J.W., McClure, B., et al., 2007.

Aircraft observations of dust and pollutants over northeast China: Insight into the meteorological mechanisms of transport. Journal of Geophysical Research-Atmospheres; 112.

Dee, D.P., Uppala, S.M., Simmons, A.J., Berrisford, P., Poli, P., Kobayashi, S., et al., 2011. The ERA-Interim reanalysis: configuration and performance of the data assimilation system. Quarterly Journal of the Royal Meteorological Society; 137: 553-597.

Duncan, B.N., Yoshida, Y., Olson, J.R., Sillman, S., Martin, R.V., Lamsal, L., et al., 2010. Application of OMI observations to a space-based indicator of NO_x and VOC controls on surface ozone formation. Atmospheric Environment; 44: 2213-2223.

Eskes, H. J., and Boersma, K. F., 2003. Averaging Kernels for DOAS Total-Column Satellite Retrievals. Atmospheric Chemistry and Physics; 3 (5): 1285–1291, doi:10.5194/acp-3-1285-2003.

Feng, Z.W., Huang, Y.Z., Feng, Y.W., Ogura, N, Zhang, F.Z., 2001. Chemical composition of precipitation in Beijing area, northern China. Water Air and Soil Pollution; 125: 345-356.

Hao, J.-M., He, K.-B., Duan, L., Li, J.-H., Wang, L.-T., 2007, Air pollution and its control in China. Frontiers of Environmental Science and Engineering in China; 1: 129-142.

He, Y., Uno, I., Wang, Z., Ohara, T., Sugirnoto, N., Shimizu, A., et al., 2007. Variations of the increasing trend of tropospheric NO_2 over central east China during the past decade. Atmospheric Environment; 41: 4865-4876.

509 IMESB, 2006. Inner Mongolia Environmental Status Bulletin 2006. Inner Mongolia
510 Environmental Protection Administration.

511 IPCC. 2007. “Climate Change 2007: The Physical Science Basis.” In Contribution of
512 Working Group I to the Fourth Assessment Report of the Intergovernmental
513 Panel on Climate Change, edited by S. Solomon, D. Qin, M. Manning, Z.
514 Chen, M. Marquis, K. B. Averyt, M. Tignor and H. L. Miller, 996. Cambridge:
515 Cambridge University Press.

516 Kajino, M., Ueda, H., Sato, K., Sakurai, T., 2011. Spatial distribution of the
517 source-receptor relationship of sulfur in Northeast Asia. Atmospheric
518 Chemistry and Physics; 11: 6475-6491.

519 Krotkov, N.A., McLinden, C.A., Li, C., Lamsal, L.N., Celarier, E.A., Marchenko, S.V.,
520 et al., 2016. Aura OMI observations of regional SO_2 and NO_2 pollution
521 changes from 2005 to 2015. Atmospheric Chemistry and Physics; 16:
522 4605-4629.

523 Lamsal, L.N., Duncan, B.N., Yoshida, Y., Krotkov, N.A., Pickering, K.E., Streets,
524 D.G., et al., 2015. U.S. NO_2 trends (2005-2013): EPA Air Quality System
525 (AQS) data versus improved observations from the Ozone Monitoring
526 Instrument (OMI). Atmospheric Environment; 110: 130-143.

527 Lee, C., Martin, R.V., van Donkelaar, A., Lee, H., Dickerson, R.R., Hains, J.C.,
528 Krotkov, N., Richter, A., Vinnikov, K., and Schwab, J.J., 2011. SO_2 emissions
529 and lifetimes: Estimates from inverse modeling using in situ and global,
530 space□based (SCIAMACHY and OMI) observations, J. Geophys. Res., 116,
531 D06304, doi:10.1029/2010JD014758.

532 Leue, C., Wenig, M., Wagner, T., Klimm, O., Platt, U., Jahne, B., 2001. Quantitative

533 analysis of NO_x emissions from Global Ozone Monitoring Experiment
534 satellite image sequences. Journal of Geophysical Research-Atmospheres; 106:
535 5493-5505.

536 Li, C., Zhang, Q., Krotkov, N. A., Streets, D. G., He, K., Tsay, S.-C., and Gleason, J. F.,
537 2010. Recent large reduction in sulfur dioxide emissions from Chinese power
538 plants observed by the Ozone Monitoring Instrument. Geophys. Res. Lett.; 37:
539 L08807, doi:10.1029/2010GL042594.

540 Li, C., McLinden, C., Fioletov, V., Krotkov, N., Carn, S., Joiner, J., Streets, D., He, H.,
541 Ren, X., Li, Z., and Dickerson, R.R., 2017. India is overtaking China as the
542 world's largest emitter of antropogenic sulfur dioxide. Scientific Report, 7,
543 14304.

544 Liu, F., Zhang, Q., Ronald, J. van der A., Zheng, B., Tong, D., Yan, L., Zheng, Y., and
545 He, K., 2016. Recent reduction in NOx emissions over China: synthesis of
546 satellite observations and emission inventories, Environ. Res. Lett., 11,
547 114002, https://doi.org/10.1088/1748-9326/11/11/114002.

548 Liu, F., Beirle, S., Zhang, Q., van der A, R.J., Zheng, B., Tong, D., and He, K., 2017.
549 NOx emission trends over Chinese cities estimated from OMI observations
550 during 2005 to 2015. Atmos. Chem. Phys., 17, 9261-9275.

551 Lu, Z., Streets, D. G., De Foy, B., Krotkov, N. A., 2013. Ozone Monitoring Instrument
552 Observations of Interannual Increases in SO_2 Emissions from Indian
553 Coal-Fired Power Plants during 2005-2012. Environmental Science &
554 Technology; 47: 13993-14000.

555 Ma, Z., Hu, X., Huang, L., Bi, J., and Liu, Y., 2014. Estimating ground-Level $PM_{2.5}$ in
556 China using satellite remote sensing. Environmental Science & Technology:

48, 7436-7444, 10.1021/es5009399.

NBS, 2013. China Energy Statistical Yearbook 2013. National Bureau of Statistics of China. China Statistics Press, Beijing.

NIW, 2017. Notice of the issuance on 'Work plan on the special treatment of SO_2 in Wuhai' by Wuhai Municipal People's Government, http://wh.nmgepb.gov.cn/wrfz/dqwrfz/zcwj1/201712/P020171211405467801681.docx,

OMI Data User's Guide, 2012, Ozone Monitoring Instrument (OMI) Data User's Guide, OMI-DUG-5.0, January 5, 2012, Produced by OMI Team.

Richter, A., Wittrock, F., Burrows, J.P., 2006, SO_2 measurements with SCIAMACHY, in Proceedings of the Atmospheric Science Conference, 8–12 May 2006, ESRIN, Frascati (CD-ROM), Eur. Space Agen., Spec. Publ. ESA SP-628.

Richter, A., Burrows, J.P., 2002. Tropospheric NO2 from GOME measurements. In: Burrows J.P., Takeucki N., editors. Advances in Space Research; 29: pp. 1673-1683.

Schaub, D., Weiss, A.K., Kaiser, J.W., Petritoli, A., Richter, A., Buchmann B., et al., 2005. A transboundary transport episode of nitrogen dioxide as observed from GOME and its impact in the Alpine region. Atmospheric Chemistry and Physics; 5: 23-37.

Seltenrich, N., 2016. A Satellite View of Pollution on the Ground Long-Term Changes in Global Nitrogen Dioxide. Environmental Health Perspectives; 124: A56-A56.

Shen, Y., Zhao, P., Pan, Y., Yu, J., 2014. A high spatiotemporal gauge-satellite merged

precipitation analysis over China. Journal of Geophysical-Research Atmospheres; 119: 3063-3075.

Shon, Z-H., Kim K-H., Song, S-K., Long-term trend in NO_2 and NO_x levels and their emission ratio in relation to road traffic activities in East Asia. Atmospheric Environment 2011; 45: 3120-3131.

Ul-Haq, Z., Tariq, S., Ali, M., 2015. Tropospheric NO2 Trends over South Asia during the Last Decade (2004-2014) Using OMI Data. Advances in Meteorology.

van der A, R.J., Mijling, B., Ding, J., Koukouli, M.E., Liu, F., Li, Q., Mao, H., Theys, N., et al., 2017. Cleaning up the air: effectiveness of air quality policy for SO_2 and NO_2 emissions in China. Atmos. Chem. Phys; 17: 1775-1789.

Wang, S., Xing, J., Chatani, S., Hao, J., Klimont Z, Cofala J, et al., 2012. Verification of anthropogenic emissions of China by satellite and ground observations. Atmospheric Environment 2011; 45: 6347-6358.

Wang, S.W., Zhang, Q., Streets D.G., He, K.B., Martin, R.V., Lamsal, L.N., et al., Growth in NOx emissions from power plants in China: bottom-up estimates and satellite observations. Atmospheric Chemistry and Physics; 12: 4429-4447.

WHO. 2000. Guidelines for Air Quality. Geneva: World Health Organization.

Yuan, Y., Liu, S., Castro, R., Pan, X., 2012. $PM_{2.5}$ Monitoring and Mitigation in the Cities of China. Environmental Science & Technology; 46: 3627-3628.

Zhang, L., Jacob, D.J., Boersma, K.F., Jaffe, D.A., Olson, J.R., Bowman, K.W., et al., 2008. Transpacific transport of ozone pollution and the effect of recent Asian emission increases on air quality in North America: an integrated analysis

using satellite, aircraft, ozonesonde, and surface observations. Atmospheric Chemistry and Physics; 8: 6117-6136.

Zhang, L., Lee, C.S., Zhang, R., Chen, L., 2017. Spatial and temporal evaluation of long term trend (2005-2014) of OMI retrieved NO_2 and SO_2 concentrations in Henan Province, China. Atmospheric Environment; 154: 151-166.

623 **Tables**

624 **Table 1.** Annual emission of different kinds of exhaust gases from 2005 to 2016 in Inner
625 Mongolia (unit: tons)

626

	Industrial SO_2 (Tons)	*Life SO_2 (Tons)*	*Total SO_2 (Tons)*	*Industrial smoke (Tons)*	*Life smoke (Tons)*	*Industrial dust (Tons)*	*Total smoke and dust (Tons)*	*NOx (Tons)*
2005	129.60	16.00	145.60	60.40	17.50	45.60	123.50	——
2006	138.40	17.30	155.70	48.80	17.20	27.00	93.00	89.82
2007	128.33	17.26	145.58	50.40	16.01	20.04	86.45	83.70
2008	125.86	17.25	143.11	42.84	15.05	20.96	78.84	104.77
2009	120.40	19.48	139.88	32.05	17.32	16.41	65.79	102.48
2010	119.30	20.11	139.41	47.59	17.10	16.04	80.73	129.38
2011	**125.02**	15.92	140.94	—	—	—	73.99	142.20
2012	124.15	14.34	138.49	—	—	—	83.30	141.89
2013	123.64	12.23	135.87	—	—	—	82.21	137.76
2014	116.71	14.53	131.24	—	—	—	102.15	125.83
2015	106.10	16.99	123.09	—	—	—	87.88	113.90

627 **Figure Captions**

628 **Figure 1.** Topographic map and the site distribution of Inner Mongolia urban.

629 **Figure 2.** The comparison between OMI VCD product and ground-based observations
630 for NO_2 (a) and SO_2 (b).

631 **Figure 3.** Spatial distribution of averaged VCD NO_2 (a), VCD SO_2 (b), surface NO_2 (c)
632 and surface SO_2 concentrations (d) from 2014 to 2016 in Inner Mongolia
633 urban agglomerations.

634 **Figure 4.** Temporal variations of VCD NO_2 (the upper), VCD SO_2 (the middle) and
635 rain rate (the lower) in Inner Mongolia. The left is the changes of monthly
636 averaged values and the right is the seasonal variation. The lines in the figure
637 represent the temporal trend.

638 **Figure 5.** Temporal variations of yearly averaged VCD NO_2 and SO_2 during the
639 period of 2005 to 2016 in Inner Mongolia urban agglomerations, along with
640 their temporal trends (dashed lines).

641 **Figure 6.** Tailpipe emission of China and Inner Mongolia including NO_2 and SO_2 (a),
642 and the energy consumption structure of Inner Mongolia (b). The energy
643 consumption in (b) includes the total, coal, fuel, gas and others. The others
644 here are clean energy including hydropower, nuclear power and so on.

645 **Figure 7.** Spatial distributions of biennial averaged VCD NO_2 and SO_2 from 2005 to
646 2016 in Inner Mongolia urban agglomerations.

647 **Figure 8.** Monthly averaged NO_2 (a), SO_2 (b), rain days and rain rate (c) and SSRD (d)
648 of Inner Mongolia urban agglomerations from 2014 to 2016.

649 **Figure 9.** Diurnal variation of surface SO_2 (a) and NO_2 (b) in five cities of Inner

650 Mongolia during the period from 2014 to 2016

651

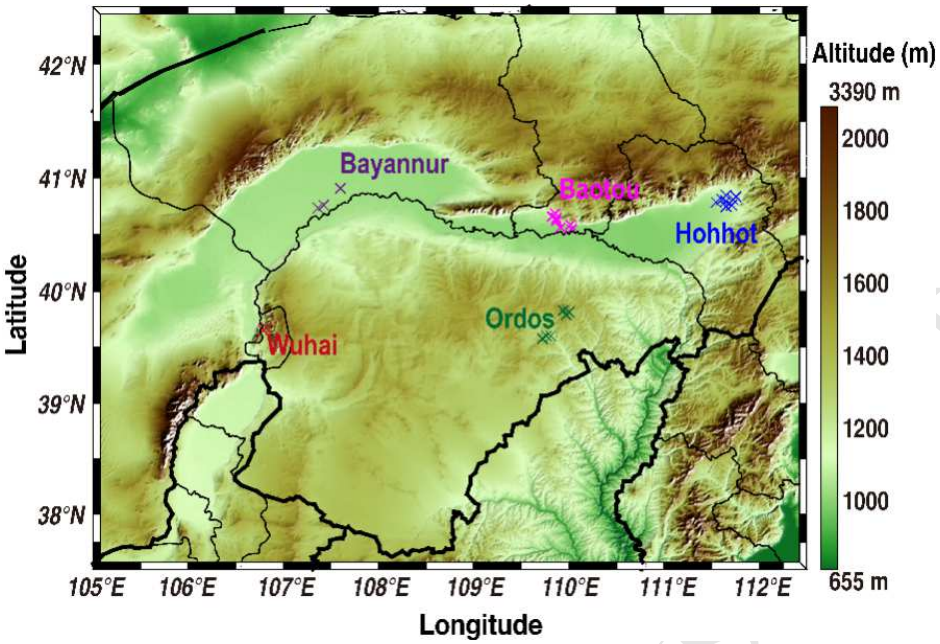

652

653 **Figure 1.** Topographic map and the site distribution of Inner Mongolia urban

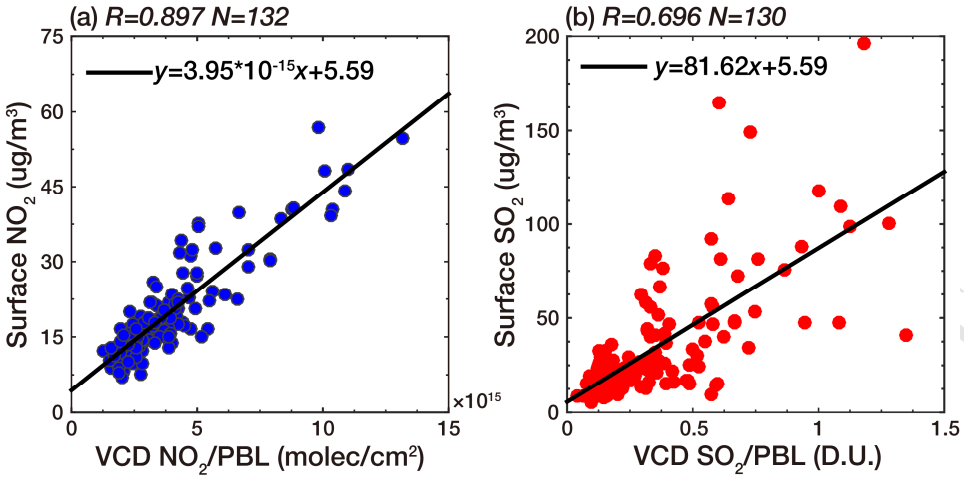

654

655 **Figure 2.** The comparison between OMI VCD product and ground-based

656 observations for NO_2 (a) and SO_2 (b).

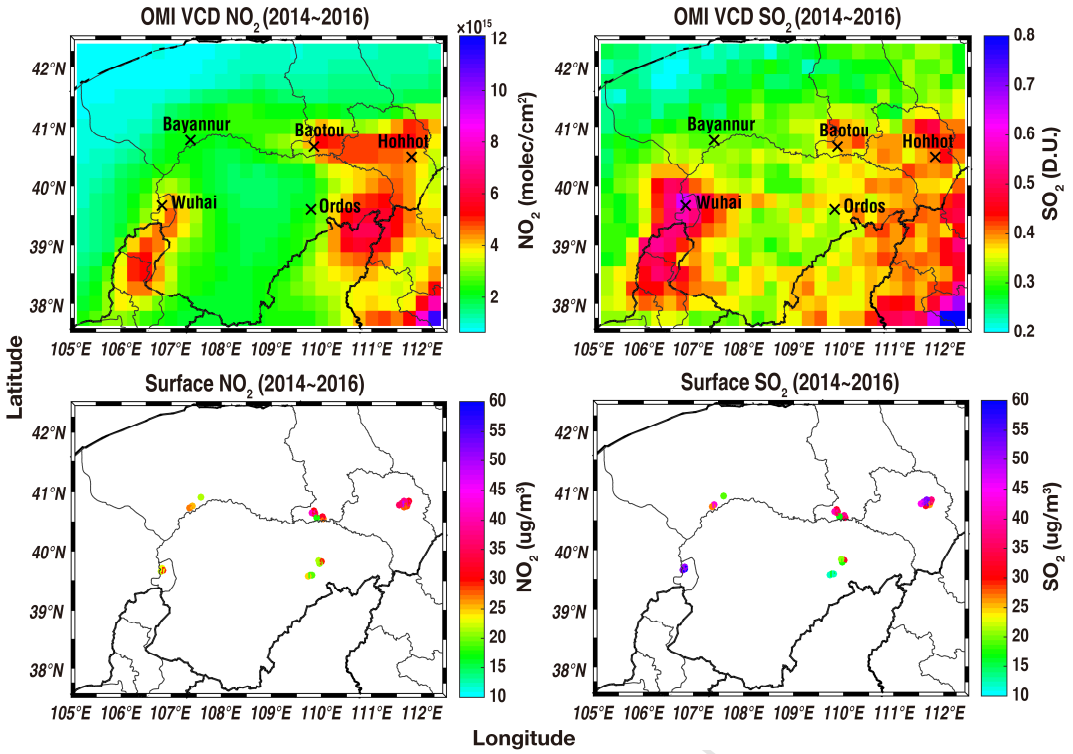

657

658 **Figure 3.** Spatial distribution of averaged VCD NO_2 (a), VCD SO_2 (b), surface NO_2

659 (c) and surface SO_2 concentrations (d) from 2014 to 2016 in Inner Mongolia urban

660 agglomerations

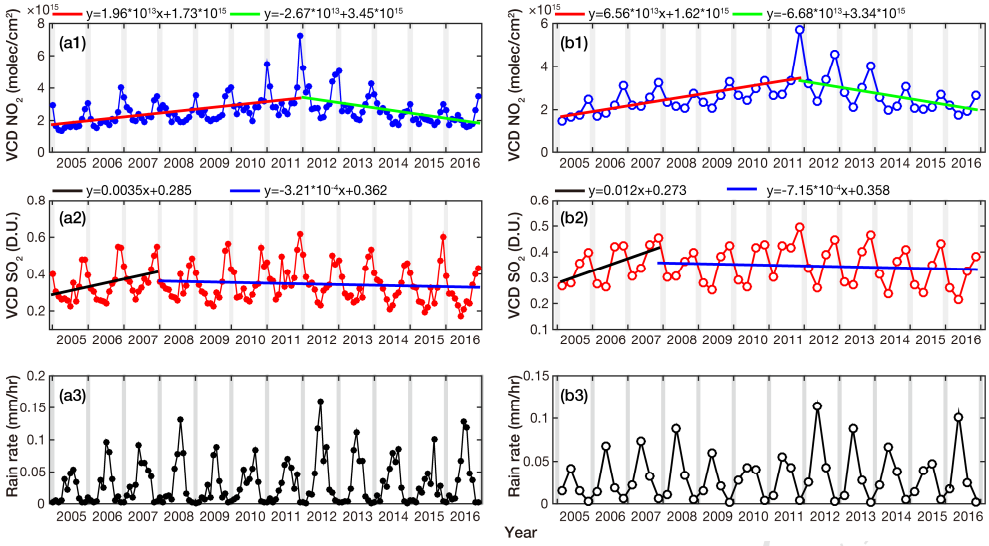

661

662 **Figure 4.** Temporal variations of VCD NO_2 (the upper), VCD SO_2 (the middle) and
663 rain rate (the lower) in Inner Mongolia. The left is the changes of monthly averaged
664 values and the right is the seasonal variation. The lines in the figure represent the
665 temporal trend

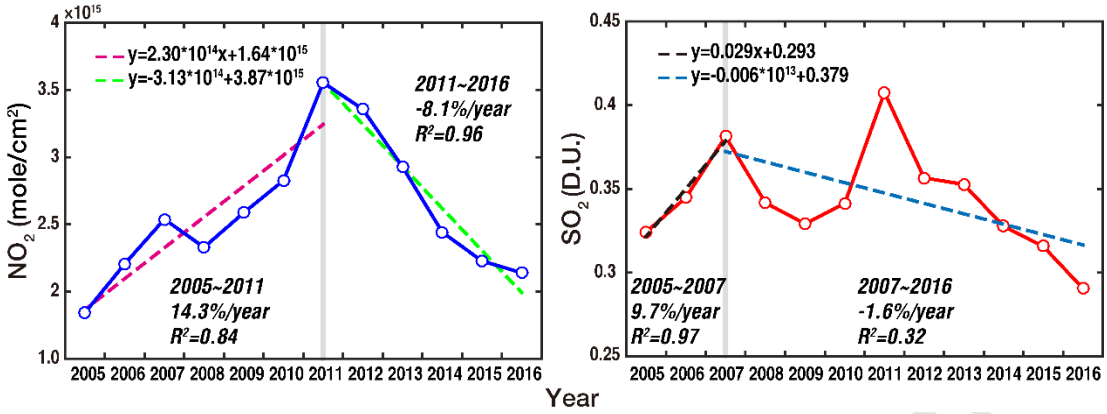

Figure 5. Temporal variations of yearly averaged VCD NO_2 and SO_2 during the period of 2005 to 2016 in Inner Mongolia urban agglomerations, along with their temporal trends (dashed lines).

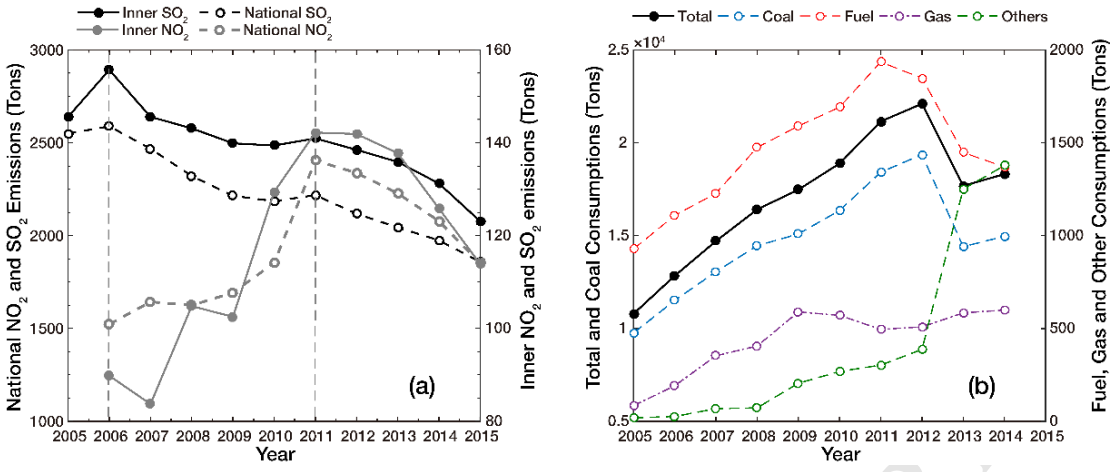

Figure 6. Tailpipe emission of China and Inner Mongolia including NO_2 and SO_2 (a), and the energy consumption structure of Inner Mongolia (b). The energy consumption in (b) includes the total, coal, fuel, gas and others. The others here are clean energy including hydropower, nuclear power and so on.

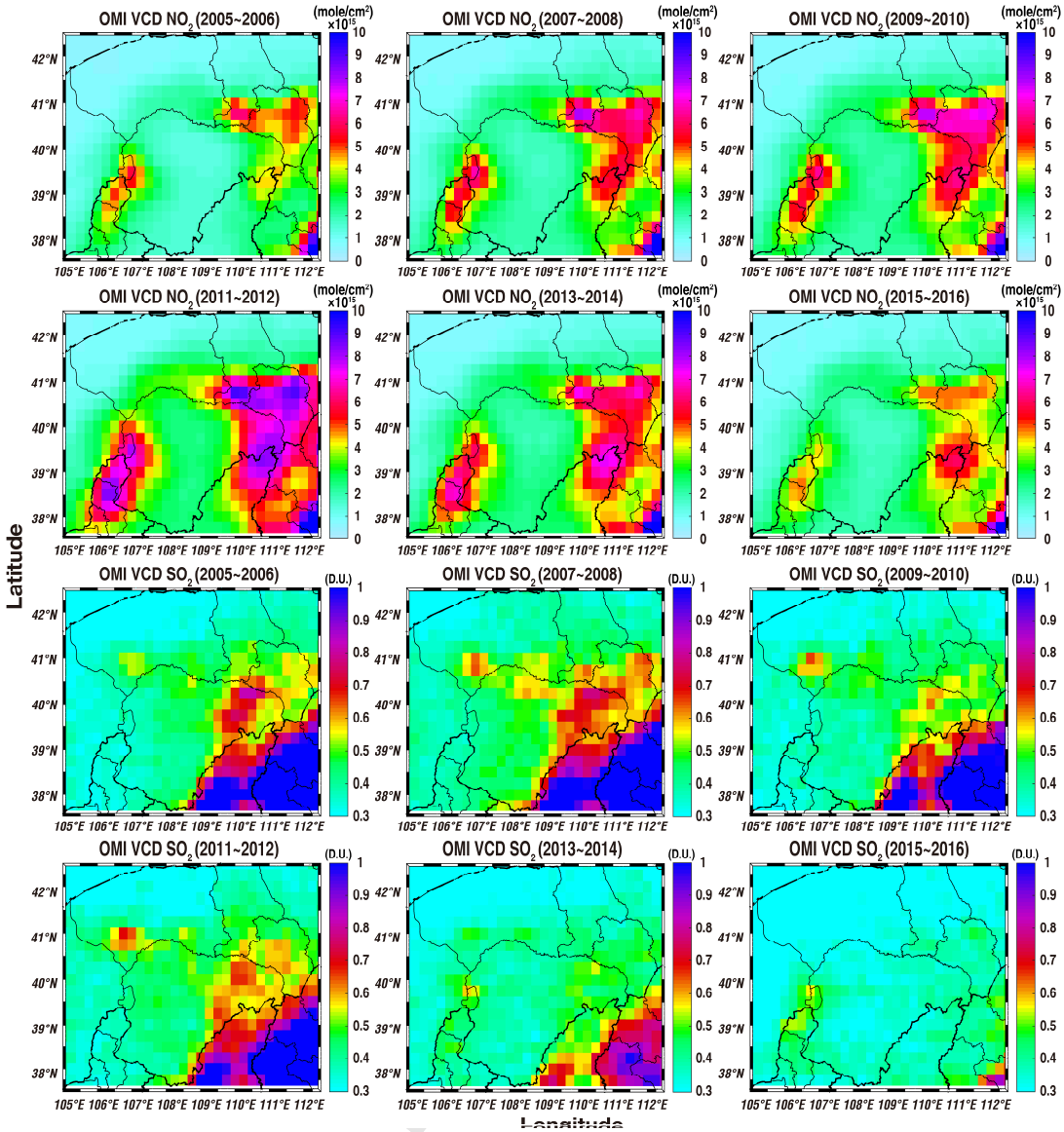

675

676 **Figure 7.** Spatial distributions of biennial averaged VCD NO_2 and SO_2 from 2005 to

677 2016 in Inner Mongolia urban agglomerations.

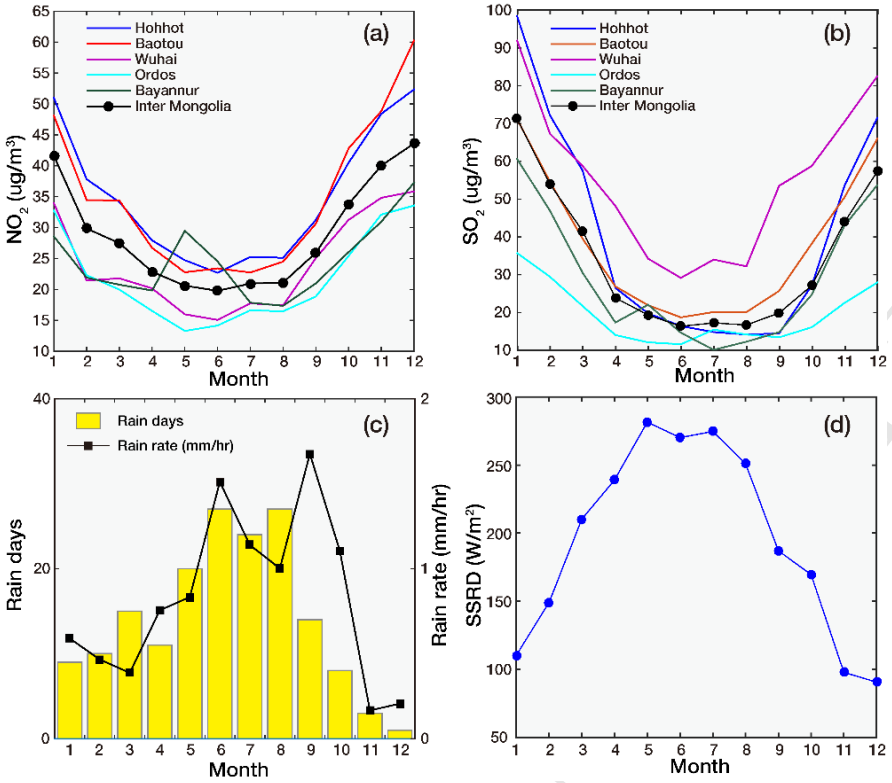

678

679 **Figure 8.** Monthly averaged NO_2 (a), SO_2 (b), rain days and rain rate (c) and SSRD (d)

680 of Inner Mongolia urban agglomerations from 2014 to 2016

681 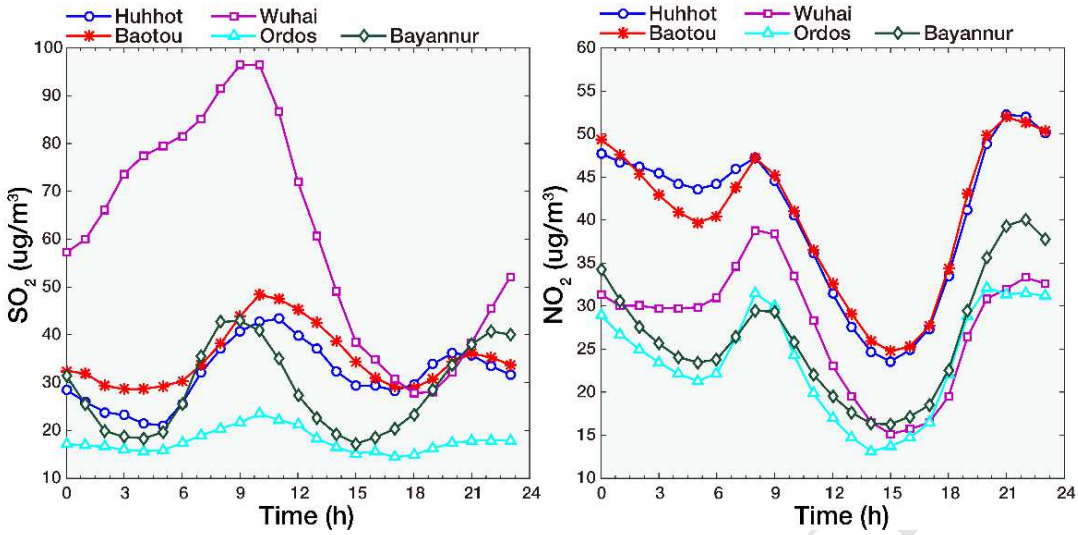

682 **Figure 9.** Diurnal variation of surface SO_2 (a) and NO_2 (b) in five cities of Inner

683 Mongolia during the period from 2014 to 2016

684

Highlights:

(1) Long-term spatial-temporal distribution of NO_2 and SO_2 amount in Inner Mongolia urban agglomerations were analyzed.

(2) Both NO_2 and SO_2 show increasing and then decreasing temporal trend, but with different turning time which are 2007 and 2011, respectively.

(3) NO_2 and SO_2 show slightly different spatial distributions, with the highest concentration in Hohhot and Baotou for NO_2 and Wuhai for SO_2.